Available online at www.sciencedirect.com
ScienceDirect
Journal of Environmental Sciences 2012, 24(1) 169–176
JOURNAL OF ENVIRONMENTAL SCIENCES
ISSN 1001-0742
CN 11-2629/X
www.jesc.ac.cn

Smog chamber study on the evolution of fume from residential coal combustion

Chunmei Geng[1,*], Kun Wang[2], Wei Wang[1], Jianhua Chen[1], Xiaoyu Liu[1], Hongjie Liu[1]

1. State Key Laboratory of Environmental Criteria and Risk Assessment, Chinese Research Academy of Environmental Sciences, Beijing 100012, China
2. Department of Environmental Science and Engineering, Tsinghua University, Beijing 100084, China

Abstract

Domestic coal stoves are widely used in countryside and greenbelt residents in China for heating and cooking, and emit considerable pollutants to the atmosphere because of no treatment of their exhaust, which can result in deteriorating local air quality. In this study, a dynamic smog chamber was used to investigate the real-time emissions of gaseous and particulate pollutants during the combustion process and a static smog chamber was used to investigate the fume evolution under simulate light irradiation. The real-time emissions revealed that the total hydrocarbon (THC) and CO increased sharply after ignition, and then quickly decreased, indicating volatilization of hydrocarbons with low molecular weight and incomplete combustion at the beginning stage of combustion made great contribution to these pollutants. There was evident shoulder peak around 10 min combustion for both THC and CO, revealing the emissions from vitrinite combustion. Additionally, another broad emission peak of CO after 30 min was also observed, which was ascribed to the incomplete combustion of the inertinite. Compared with THC and CO, there was only one emission peak for NOx, SO_2 and particular matters at the beginning stage of combustion. The fume evolution with static chamber simulation indicated that evident consumption of SO_2 and NOx as well as new particle formation were observed. The consumption rates for SO_2 and NOx were about 3.44% hr^{-1} and 3.68% hr^{-1}, the new particle formation of nuclei particles grew at a rate of 16.03 nm/hr during the first reaction hour, and the increase of the diameter of accumulation mode particles was evident. The addition of isoprene to the diluted mixture of the fume could promote O_3 and secondary particle formation.

Key words: residential coal combustion; smog chamber; new particle formation; emission characteristics
DOI: 10.1016/S1001-0742(11)60741-9

Introduction

It is well known that residential coal is widely used in China. Residential coal combustion is mainly carried out in small stoves under poor combustion conditions and without any emission control. This kinds of combustion emitted high particulate matter, CO, SO_2, PAHs and other air pollutants, which lead to serious air pollution and health danger (Guo et al., 2004; Jacobson, 2001).

One major concern about the evolution of plume from combustion sources was focused on primary particle emission and the secondary aerosol formation in the diffusion process (McMurry et al., 1981; Brock et al., 2002). Early researches have demonstrated that SO_2 emissions from power plants resulted in downwind formation of fine, sulfur-containing particles (Hewitt, 2001; Davis et al., 1979). Evolution of the particles in power plant plumes under cloud-free conditions showed that the size distributions of the particles was generally consistent with aerosols accumulated by a condensation process (Springston et al., 2005).

Another focus concern about the evolution of plume from combustion sources was the elevated ozone level resulted from these sources. During the diffusion of the plumes, high concentration of O_3 may be generated. For example, only a single power plant can emit more NOx than a mid-sized city, which will lead to high O_3 concentrations downwind (Springston et al., 2005). The content of the plume is closely related with O_3 production efficiency, which is observed to decrease with increasing NOx emissions and is higher in regions with high biogenic isoprene emissions (Luria et al., 2000; Ryerson et al., 2001).

Above mentioned researches focused on coal combustion in power plant. For residential coal combustion, it is especially important when considering population exposure (Lighty et al., 2000). Most of previous studies only focused on the emissions of PAHs and fine particles from domestic stoves (Chen et al., 2004). In this work, the emission characteristics of various pollutants (including NOx, SO_2, CO and particular matters) from a typical kind of domestic coal stove were investigated, and preliminary study of the photochemical evolution of the fume was also carried out under two typical simulation conditions.

1 Methods

1.1 Coal samples and stove

Raw coal was purchased from state-own coal mines

* Corresponding author. E-mail: gengcm@craes.org.cn

(Ningxia, China). Its characteristics are shown in Table 1. The coal was broken into pieces of 5–8 cm diameter before being used. The coal-stove, which is widely used for cooking and heating in China, was purchased from the grocery market.

Table 1 Analytical characteristic of the coal (dry basis)

Industrial analysis		Elemental analysis	
Moisture	1.3%	Carbon	62.68%
Volatile matter	23.28%	Hydrogen	2.16%
Ash	19.74%	Nitrogen	0.62%
Fixed carbon	55.68%	Oxygen	9.6%
Higher heating value	19.85 MJ/kg	Sulfur	0.36%

1.2 Experimental system

The schematic diagram of the dilution tunnel and smog chamber system is shown in Fig. 1. The dilution tunnel system was used to sample and dilute fume from residential coal combustion. The dilution tunnel consists of two main parts made of stainless steel including an orthogonal pipe and a cylindrical tunnel. During sampling process, all flue gases were introduced into dilution tunnel and mixed with filtered air. The flow rate of the suction fan was controlled by Venturic tube and fixed at 5800 L/min. To avoid particle losses, a dynamic dilutor was used to introduce the flue gas into the smog chambers. The principle of the dynamic dilutor is based on ejection dilution. Purified pressurized dilution air flows at high speed around an ejector nozzle and caused a pressure drop which draws a sample through the nozzle. The raw sample is instantaneously diluted as it mixes with the dilution airflow. During the experiments, the flow rate of the diluted flue gas into smog chamber was fixed at 100 L/min.

1.3 Smog chamber system

Two smog chambers were used: dynamic smog chamber for real-time measurement of gaseous and particulate pollutant during the combustion process; static smog chamber for study the evolution of fume. The smog chambers, which were made of FEP-Teflon film, were all cylindrical shape and the total volumes were 2.0 and 0.2 m^3 for static and dynamic smog chamber, respectively. The wall loss rate of particle was tested to be about 0.264 hr^{-1} for static smog chamber. All the particle concentrations measured in experiments were corrected based on the loss rate. For dynamic smog chamber, the flow direction was from up to down and the overall remaining time was only 2 min, and this imply that the wall loss can be neglect.

For static smog chamber, 16 black light lamps (Philips TUV 36W/G36 T8, Holland) were equipped to provide ultraviolet light with maximum emission wavelength of 365 nm. The inside wall and floor of the box are covered with aluminum foil to increase the reflection of ultraviolet light for strengthening the light efficiency.

The gaseous pollutants including CO, NOx, SO_2, O_3 and total hydro carbon (THC) were measured using gas analyzers (48i, 42i, 43i, 49i, 51C, Thermo Electronic, USA). The particles were determined using Model 3090 Engine Exhaust Particle Sizer^{TM} Spectrometer (TSI-EEPS 3090, USA).

1.4 Combustion process

Raw coal samples were ignited in the stove using pre-weighed charcoal (0.5 kg). To estimate the interference of charcoal combustion, charcoal was burned without adding any coal to determine how long the fume from the charcoal fire would persist. Black smoke appeared only after the charcoal was ignited and no obvious smoke could be seen after igniting period. The results showed that both gaseous and particulate emissions after the smoking period of charcoal combustion were very small and could be neglected. Consequently, the raw coal samples (1.0 kg for each experiment) were put into the stove until smoking from charcoal combustion stopped. Dilution and sampling started when the raw coal samples were put into the stove and ended until the combustion finished. This process lasted for about one hour.

2 Results and discussion

2.1 Fume emission during combustion process

When the coal chunks were added into the stove, they immediately began to give off odors and rapidly caught fire. With further increasing temperature, combustible volatiles as well as tarry substances and reactive carbonaceous char were vaporized. This exothermic oxidation combustion in gas phase started and lasted until the flux of combustible

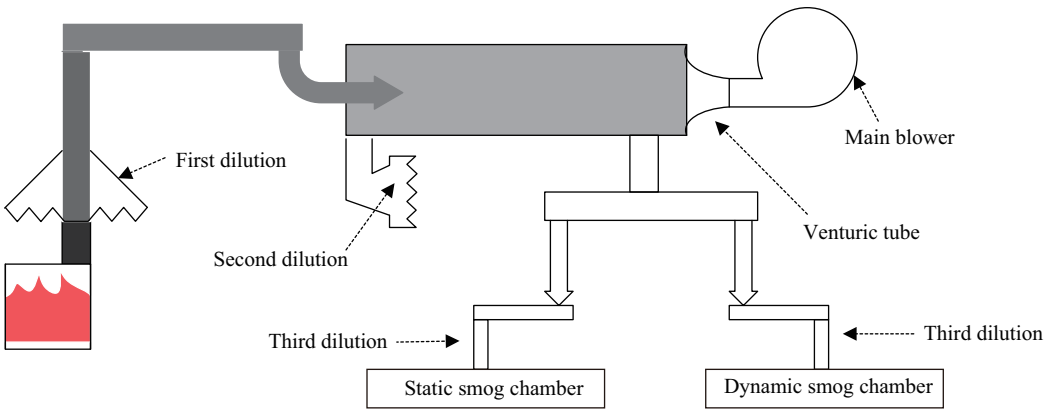

Fig. 1 Sketch diagram of the dilution tunnel and smog chamber system.

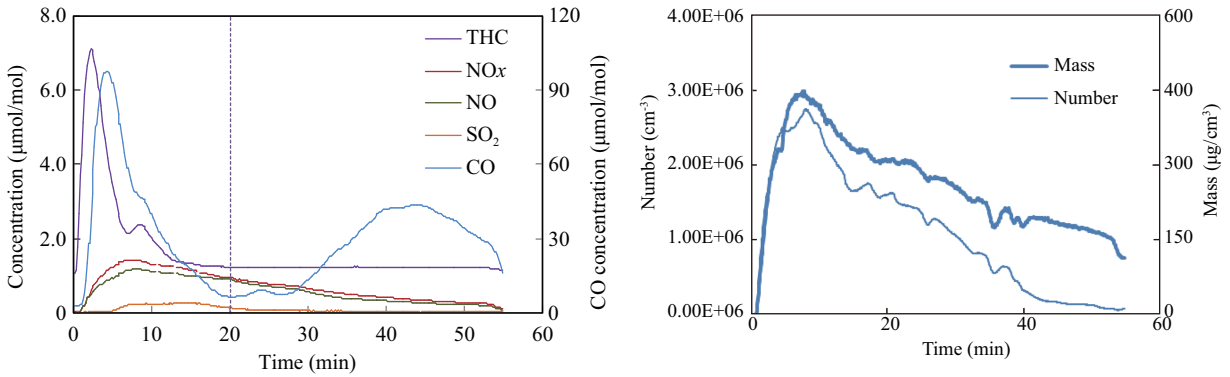

Fig. 2 Gases and particle emission concentration during combustion process.

Table 2 Comparision of emission factors for coal stoves

Number	CO	SO_2	NOx	C_mH_n	PM	Reference
1	53.30	0.41	1.45	1.72	6.29 (PM_{10}) 3.30 ($PM_{2.5}$)	This study
2	–	–	–	–	0.78–11.06 ($PM_{2.5}$)	Liu et al., 2007
3	–	–	1.88	–	1.3 (TSP)	Yu et al., 2008
4	–	11.54	–	–	–	Sun and Wu, 1998
5	78.05	1.47	0.50	1.51	0.71 (TSP) 0.31 (PM_{10}) 0.10 ($PM_{2.5}$)	Tang et al., 2002

volatiles drops below the level needed to maintain exothermic oxidation combustions. Subsequently, the solid-phase combustion started and very little smoke was observed. The real time concentrations of CO, THC and particular matters (PMs) could well reflect the above combustion processes (Fig. 2). The sharply increase of THC just after igniting the coal chunks implied volatilization of hydrocarbons with low molecular weight. The extremely high concentration of THC vaporized from heating the coal chunks and the relatively low temperature at the beginning combustion stage favored incomplete combustion, and resulted in sharply increase of CO formation as shown in Fig. 2. With continuance of combustion process, the THC and CO sharply decreased due to depletion of the volatile hydrocarbons. There was an evident shoulder peak emission of THC and CO around 10 min, implying volatilization of hydrocarbons with relatively high molecular weight as the temperature further increased during the combustion process. Additionally, another broad emission peak of CO after 30 min was also observed, which was ascribed to the incomplete combustion of the inertinite. The three combustion processes identified by the emission characters of THC and CO agreed well with the results of Smith et al. (1981) who investigated the combustion processes by using pulverized coal. Compared with THC and CO, there was only one emission peak for NOx, SO_2 and PMs at the beginning stage of combustion, and they gradually decreased after their emission peaks, indicating NOx and SO_2 might be the dominant precursors for the PMs.

The summary of emission factors for CO, SO_2, NOx, CmHn and PM in this study and in references are listed in Table 2. Only the same kind of residential coal-stove were included in Table 2. Because the emission factors for PM in references were obtained from membrane sampling, the same method was used for the data in this study. As shown in Table 2, the emission factors in this study were similar to those references.

2.2 Static smog chamber study on fume evolution under irradiation

To eliminate particles with large size into the static chamber, the fume from the stove was firstly introduced into the reaction bag via a relative long tube (length 2 m, diameter 10 mm). Then the reaction bag was shifted to another room and put into the static chamber. The time interval from sampling completion to starting the irradiation experiment was about 30 min. Due to different proportion of dilution and particles congregation and deposition during the process of preparation, the concentrations of gases and particles were less than that in real time measurement, especially for particles.

2.2.1 Gaseous phase

The photochemical evolutions of NOx, NO, NO_2, THC and SO_2 are shown in Fig. 3. The gradually decrease of the primary gaseous pollutants of NO, THC and SO_2 as well as increase of NO_2 under the UV light irradiation were ascribed to photochemical consumption and production of them. The initial amount of NO_2 in the chamber could react with H_2O on the wall surface of chamber and particles, and resulted in formation of HONO which would generate OH radicals under weak light irradiation, and hence initiated photochemical reactions in the chamber. The OH radicals generated in the chamber could initiate oxidation of the THC, SO_2 and NO_2, and degradation of THC would form organic peroxy radicals and HO_2 which could fast convert NO to NO_2 with OH radical reforming, and hence, sustained the photochemical reactions in the chamber. The consumption rates for SO_2 and NOx in the

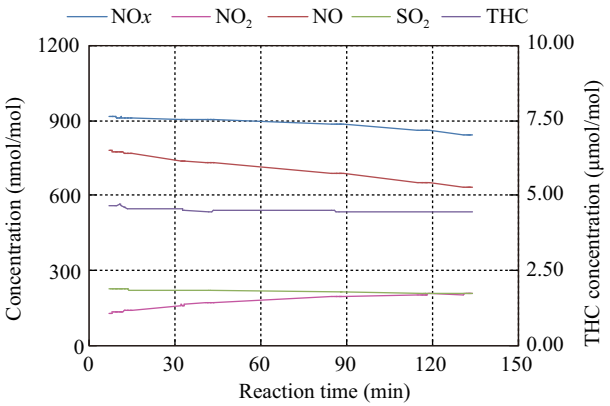

Fig. 3 Variation of SO_2 and NOx concentration in smog chamber under irradiation.

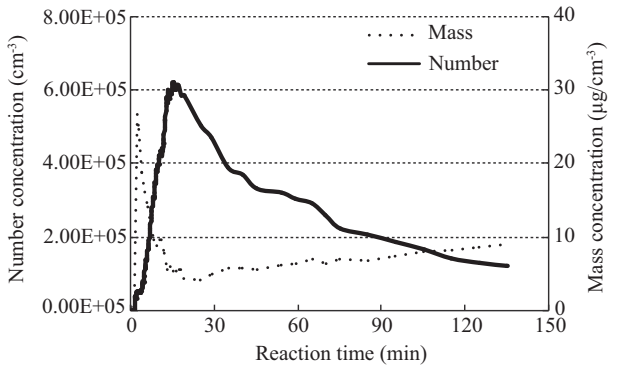

Fig. 4 Variation of total number and mass concentration of particles in the smog chamber during irradiation.

chamber were 3.44% hr^{-1} and 3.68% hr^{-1}. It should be mentioned that O_3 was not observed in the chamber. It is well known that mixture of NOx and hydrocarbons under UV light irradiation can produce O_3, however, O_3 was not observed in the chamber under present experimental conditions. O_3 is solely from NO_2 photolysis producing ground state oxygen atom (O^3P) which reacts rapidly with O_2 to form O_3. O_3 also can be consumed via different reaction channels, such as wall loss, reactions with NO and unsaturated hydrocarbons etc. When NO concentration is high, the titration reaction of NO with O_3 will dominate O_3 loss, which is the well known reason for the extremely low O_3 concentration (even zero) in urban areas during night and in the plume of power plants. In this study, although the fume from the stove was diluted to some extent, NO concentration was still higher than 600 ppbv, O_3 formed via photolysis of NO_2 could be quickly consumed by the titration reaction of NO.

2.2.2 Particular phase

The variations of total number and mass concentration of particles along with time are shown in Fig. 4. Before irradiation, the particle concentrations were just above detection limit. Under irradiation of UV light, particle formation and followed condensation were observed. For mass concentration, the total mass concentration reached its peak just after irradiation of 2 min. But for number concentration, after irradiation of about 16 min, the total number concentration reached its peak (6.13×10^5 cm^{-3}). Then the total concentrations decreased with time.

The size distribution changed dramatically and the early period around irradiation beginning can be seen in Fig. 5. The changes in nuclei mode and accumulation mode were different. The size distribution at different time is shown in Fig. 6 and particle diameter (D_p) at peaks is listed in Table 3. Before irradiation, there was a peak at 124.08 nm (3.60×10^2 cm^{-3}) and a peak at 9.31 nm (2.08×10^3 cm^{-3}). At 1 min after irradiation, the numbers of particles in accumulation mode increased, which was from the new particle formation and its following accumulation in

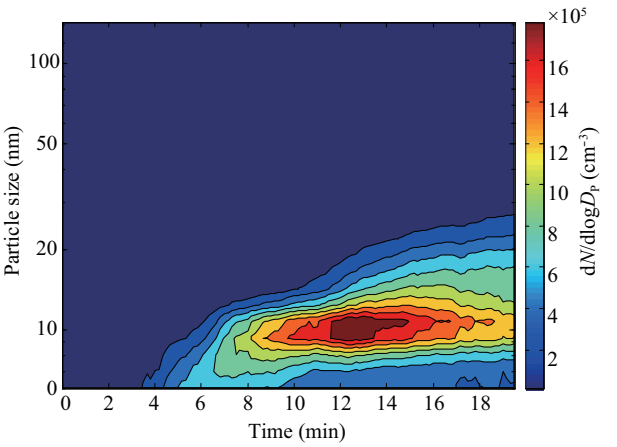

Fig. 5 Variation of particle size distribution in the smog chamber during early irradiation period (0–20 min).

Table 3 Particle size distribution during irradiation

Reaction time (min)	Aitken nuclei mode				Accumulation mode	
	First peak		Second peak		First peak	
	Size (nm)	dN/dlogD_p (cm^{-3})	Size (nm)	dN/dlogD_p (cm^{-3})	Size (nm)	dN/dlogD_p (cm^{-3})
0	9.31	2.08×10^3	–	–	124.08	3.60×10^2
1	10.75	9.40×10^3	–	–	80.58	9.10×10^4
3	6.04	2.28×10^5	–	–	80.58	8.10×10^4
5	6.04	6.92×10^5	–	–	80.58	5.01×10^4
7	8.06	9.95×10^5	–	–	93.06	2.82×10^4
10	9.31	1.67×10^6	–	–	93.06	1.01×10^4
15	10.75	1.70×10^6	–	–	93.06	2.63×10^4
20	10.75	1.31×10^6	–	–	93.06	5.73×10^3
30	10.75	7.52×10^5	–	–	107.46	5.39×10^3
60	10.75	3.30×10^5	22.07	6.03×10^5	124.409	2.52×10^3
95	10.75	1.93×10^5	33.98	3.29×10^5	–	–
135	10.75	7.23×10^4	45.3	1.12×10^5	–	–

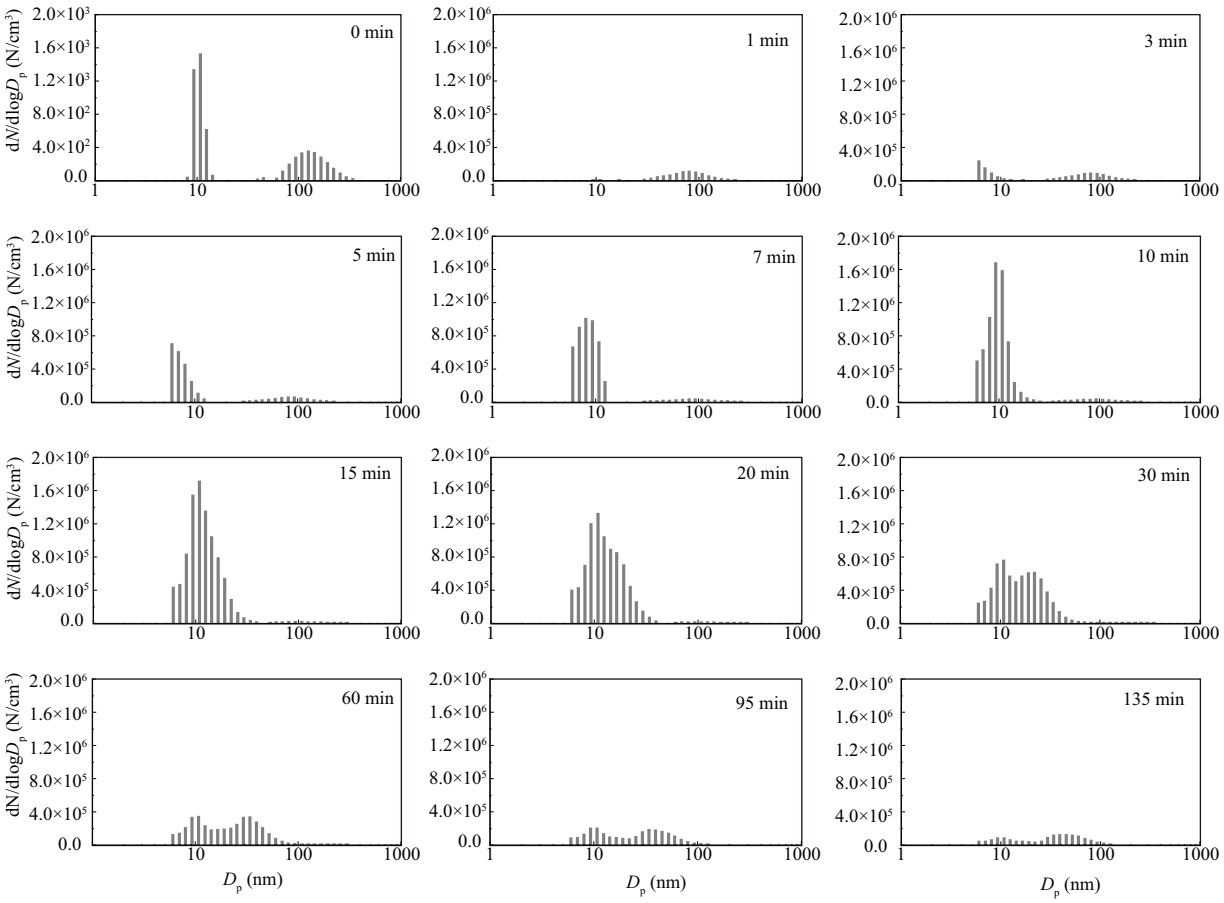

Fig. 6 Particle size distributions at different reaction time in the smog chamber.

existed particles. With the experiments going on, obvious accumulation of new particle in nuclei mode could be seen. The diameter of particles grew at a rate of 16.03 nm/hr during the first reaction hour and two peaks at nuclei mode were formed after 60 min irradiation. For accumulation mode, the increase of the diameters at peaks also can be seen and no independent peak existed after 60 min. With these diameters increased, the whole number concentration decreased, which were caused partly by the ultrafine particle's condensation on big particles and the coalescence between particles, and partly by the wall losses.

2.3 Static smog chamber study on the evolution process of fume added with isoprene

It is well documented that O_3 production in power plant plumes was delayed until the plumes were quite diluted (Luria et al., 1999), and O_3 production is known to be enhanced when the plumes mix with external sources of VOCs, such as urban plumes (Luria et al., 2000). Therefore, in this study, isoprene, which is the most abundant VOCs from natural sources, was selected as external VOCs to simulate the photoreaction of fume with natural VOCs after dilution in air. Additionally, isoprene is very reactive and can promote the evolution process for fume from residential coal combustion.

As mentioned above, high NO concentration resulted in the inhibition of O_3 accumulation. To investigate the evolution process of the flue gas after it diffused and mixed with ambient air mass, sampled fume was firstly diluted to half of the original concentration with zero air. After the fume was diluted, THC concentration was 1.50 μmol/mol. Then using zero air, isoprene (liquid) was introduced into the smog chamber. Before irradiation, each gas concentration was as follows: THC 4.65 μmol/mol, CO 12.93 μmol/mol, NO*x* 263 nmol/mol, NO 230 nmol/mol, O_3 0 nmol/mol, NO_2 33 nmol/mol, SO_2 157 nmol/mol.

2.3.1 Gas phase

The evolutions of NO*x*, SO_2, THC and O_3 during irradiation are illustrated in Fig. 7. Compared with the original fume, the decrease of SO_2 and NO*x* were more evident, with consumption rates of 16.66% hr^{-1} and 29.15% hr^{-1}, respectively. For THC, as extra isoprene was introduced into the chamber and extremely high THC concentration, its decrease rate was as low as that of the original fume, indicating overdose of THC in the chamber. Because of the addition of the high reactive isoprene, more peroxy radicals would be formed in the chamber and resulted in high conversion rate of NO to NO_2. The fast production of NO_2 could accelerate HONO formation via heterogeneous reactions as mentioned in above, and resulted in higher concentration of OH radicals which further facilitate SO_2 oxidation. In addition, the extremely high concentration of isoprene introduced in the chamber could compete with NO for reaction with O_3, and produce extra OH radical for further consuming NO*x* and SO_2. Although the fume was further diluted, the extremely high initial NO concentration

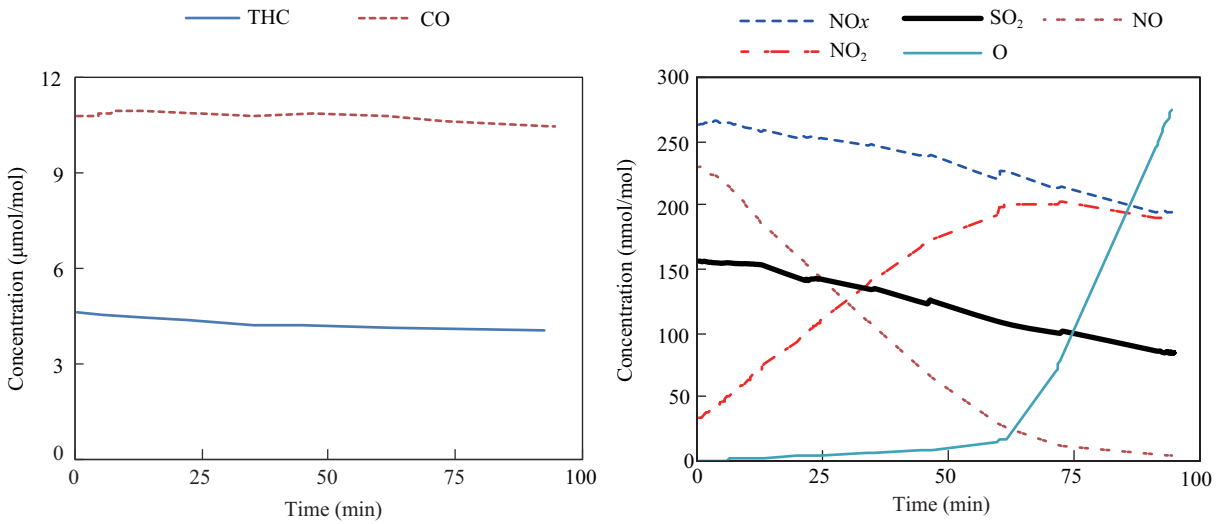

Fig. 7 Variation of gas concentrations of fume with isoprene in smog chamber under irradiation.

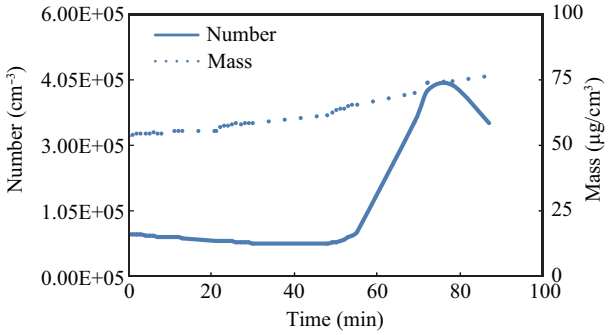

Fig. 8 Variation of particle mass and number concentrations of fume with isoprene under irradiation.

(230 nmol/mol) still suppresses O_3 accumulation during 55 min irradiation. Whereas O_3 concentration was built up quickly as NO concentration dropped to be about 40 nmol/mol, which is around the ambient level in urban areas. This result indicated that the domestic coal stove could emit large amount of NO and would result in high O_3 during dilution process.

2.3.2 Particular phase

The variations of total number and mass concentration of particles along with time are shown in Fig. 8. It is interesting to note that the initial mass concentration of particles was much higher than that of the original fume, indicating the dark reaction of the introduced isoprene with the existing particles might be the reason for the increased mass concentration. In contrast to the irradiation experiment of the original fume, neither the number of particles nor the mass concentration increased sharply as irradiation started. Instead of sharp increase for the original fume, the mass concentration in the mixture of original fume with addition of isoprene increased gradually, while the number of particles even decreased at early stage of irradiation and increased dramatically at about 55 min which was coincident with the point of O_3 quickly accumulation. Therefore, the reaction of isoprene with O_3 was an important source for these new particles. Although the number of particles increased dramatically at about 55 min, the increase rate of mass concentration kept steady, implying the increased mass concentration was mainly ascribed to the oxidation of inorganic gaseous (such as SO_2 and NOx) or hydrocarbons with high molecular weight (such as PAHs).

The size distributions at different time are shown in Fig. 9 and D_p at peaks is listed in Table 4. Before irradiation, there was a peak at 93.1 nm (2.54×10^5 cm^{-3}) and a peak at 10.75 nm (1.41×10^3 cm^{-3}). For nuclei mode, the maximum number concentration at peak appeared after 70 min irradiation. Then the second peak formed, which

Table 4 Particle size distribution during irradiation

Reaction time (min)	Aitken nuclei mode				Accumulation mode	
	First peak		Second peak		First peak	
	Size (nm)	dN/dlogD_p (cm^{-3})	Size (nm)	dN/dlogD_p (cm^{-3})	Size (nm)	dN/dlogD_p (cm^{-3})
0	10.75	1.41×10^3	–	–	93.1	2.54×10^5
10	9.31	8.23×10^2	–	–	93.1	2.42×10^5
30	8.06	2.70×10^3	–	–	93.06	2.16×10^5
45	6.04	3.61×10^4	–	–	107.5	1.94×10^5
55	6.04	1.19×10^5	–	–	107.5	1.83×10^5
70	10.75	9.52×10^5	–	–	107.5	1.65×10^5
80	10.75	8.65×10^5	16.5	5.58×10^5	124.1	1.51×10^5
87	10.75	5.05×10^5	22.1	4.23×10^5	124.1	1.34×10^5
94	10.78	2.70×10^5	29.4	3.44×10^5	124.1	1.26×10^5

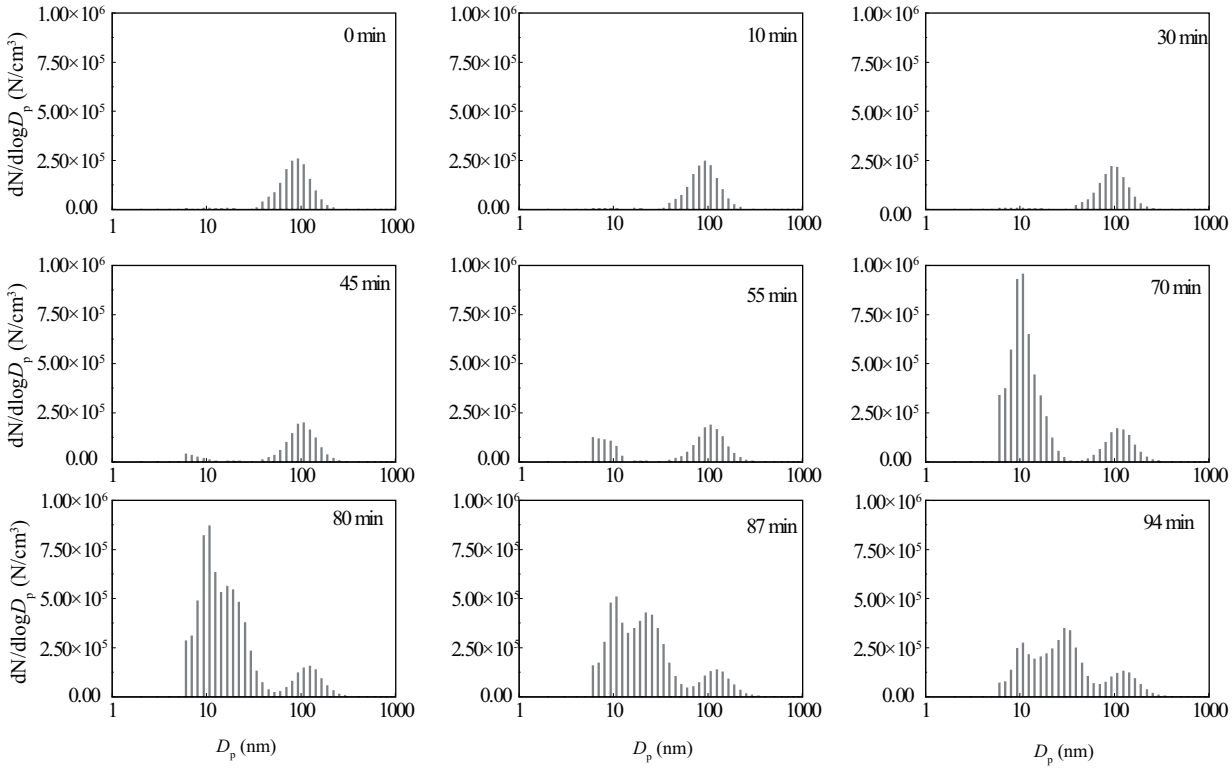

Fig. 9 Particle size distributions at different reaction time for fume with isoprene in the smog chamber.

were the results of the ultrafine particle's condensation on big particles and the coalescence between particles. For accumulation mode, the number concentration remained in high concentration level ($\times 10^5$ cm^{-3}) and the peak increased from 93.1 to 124.1 nm. This also demonstrated the existence of new particle formation and its adsorption to big particles.

3 Conclusions

One typical kind of coals in China (Ningxia, Yinchuan) was selected to study the emission characteristics, as well as to explore the evolution of fume from coal combustion. Using smog chambers, the evolution of fume emitted from the first stage of coal combustion were studied as a single source. The photoreaction of fume with active VOCs resulted in net O_3 accumulation as well as new particle formation and its aggregation. It can be confirmed that coal combustion pollutants may serve as an important source of O_3 and secondary ultrafine particles, especially in rural areas where large amount of raw coal are burned and large amount of reactive VOCs from plant are released.

Acknowledgments

This work was supported by the Central Public-Interest Scientific Institution Basal Research Fund (No. 2009KYYW01), the National Natural Science Foundation of China (No. 40705043), and the Open Foundation of Environmental Simulation and Pollution Control State Key Laboratories (Peking University). We are grateful to Prof. Ge Maofa and Prof. Mu Yujing for their valuable advice regarding experimental design and article writing.

References

Brock C A, Washenfelder R A, Trainer M, Ryerson T B, Wilson J C, Reeves J M et al., 2002. Particle growth in the plumes of coal-fired power plants. *Journal of Geophysical Research*, 107(D12): 4155. DOI: 10.1029/2001JD001062.

Chen Y J, Bi X H, Mai B X, Sheng G Y, Fu J M, 2004. Emission characterization of particulate/gaseous phases and size association for polycyclic aromatic hydrocarbons from residential coal combustion. *Fuel*, 83(7-8): 781–790.

Davis D D, Heaps W, Philen D, McGee T, 1979. Boundary layer measurements of the OH radical in the vicinity of an isolated power plant plume: SO_2 and NO_2 chemical conversion times. *Atmospheric Environment*, 13(8): 1197–1203.

Guo H, Wang T, Simpson I J, Blakeb D R, Yu X M, Kwoka Y H et al., 2004. Source contributions to ambient VOCs and CO at a rural site in eastern China. *Atmospheric Environment*, 38(27): 4551–4560.

Hewitt C N, 2001. The atmospheric chemistry of sulphur and nitrogen in power station plumes. *Atmospheric Environment*, 35(7): 1155–1170.

Jacobson M Z, 2001. Strong radiative heating due to the mixing state of black carbon in atmospheric aerosols. *Nature*, 409(6821): 695–697.

Lighty J S, Veranth J M, Sarofim A F, 2000. Combustion aerosols: factors governing their size and composition and implications to human health. *Journal of Air & Waste Management Associate*, 50: 1565–1618.

Liu Y, Zhang Y X, Wei Y J, Dou H, Gu D S, Zeng L M et al., 2007. Measurement of emission factors of carbonaceous aerosols from residential coal combustion. *Acta Scientiae Circumstantiae*, 27(9): 1409–1416.

Luria M, Tanner R L, Imhoff R E, Valente R J, Bailey E M,

Mueller S F, 2000. Influence of natural hydrocarbons on ozone formation in an isolated power plant plume. *Journal of Geophysics Research*, 105(D7): 9177–9188.

Luria M, Valente R J, Tanner R L, Gillani N V, Imho R E, Mueller S F et al., 1999. The evolution of photochemical smog in a power plant plume. *Atmospheric Environment*, 33: 3023–3036.

McMurry P H, Rader D J, Stith J L, 1981. Studies of aerosol formation in power plant plumes I – Growth laws for secondary aerosols in power plant plumes: implications for chemical conversion mechanisms. *Atmospheric Environment*, 15(10-11): 2315–2327.

Ryerson T B, Trainer M, Holloway J S, Parrish D D, Huey L G, Sueper D T et al., 2001. Observations of ozone formation in power plant plumes and implications for ozone control strategies. *Science*, 292: 719–723.

Smith S E, Neavel R C, Hippo E J, Miller R N, 1981. DTGA combustion of coals in the Exxon coal library. *Fuel*, 60: 458–462.

Springston S R, Kleinman L I, Brechtel F, Lee Y N, Nunnermacker L J, Wang J, 2005. Chemical evolution of an isolated power plant plume during the TexAQS 2000 study. *Atmospheric Environment*, 39(19): 3431–3443.

Sun Z, Wu Y, 1998. Study of emission factor of SO_2 due to coal-burning in Shanghai. *Shanghai Environmental Sciences*, 7(12): 15–18.

Tang X, Chen F, Zhang Y, Chai F H, Yang M Z, Wang G C et al., 2002. Analysis of causes and sources of atmospheric pollution in Beijing (Report). Beijing Municipal Environmental Protection Bureau.

Yu J P, Cui P, Wang W Y, 2008. Estimation on SO_2, NOx and TSP emissions from energy consumption for non-production purpose in rural areas of China. *Geographical Research*, 27(3): 547–555.